Report

Current Biology

Tissue-specific regulation of volatile emissions moves predators from flowers to attacked leaves

Graphical abstract

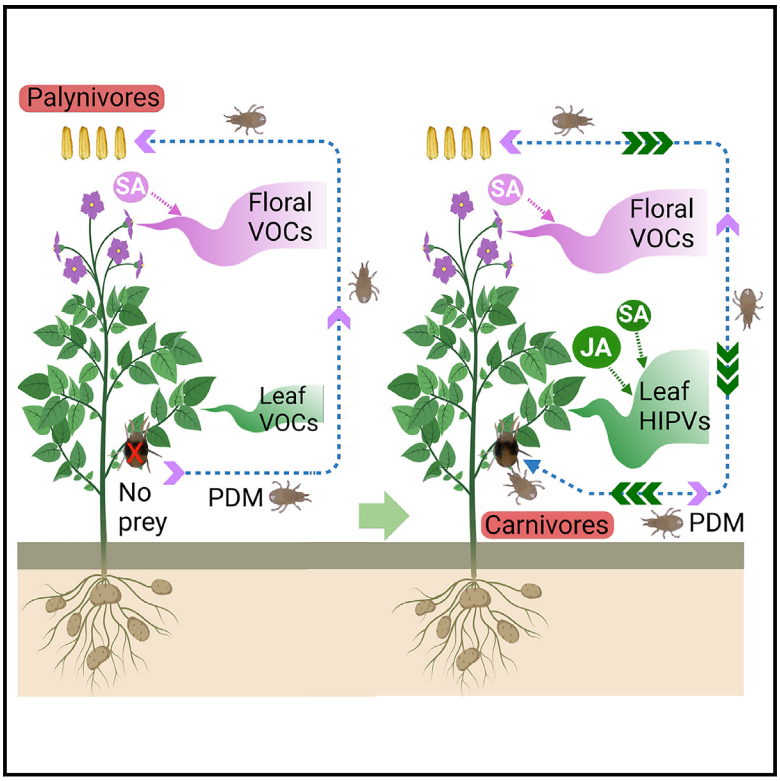

Highlights

- Within-plant up-down movement switches predators from palynivory to carnivory
- Movement of predators is mediated by organ-specific emissions of plant volatiles
- Organ-specific emissions of plant volatiles are mediated by JA and SA signaling

Authors

Asim Munawar, Yi Xu, Amr S. Abou El-Ela, ..., Zengrong Zhu, Ian T. Baldwin, Wenwu Zhou

Correspondence

wenwuzhou@zju.edu.cn

In brief

Zhou et al. observe that the within-plant "up-down" movement of predatory mites on wild potato plants switches their feeding behavior from palynivory to carnivory. This movement behavior is mediated by the organ-specific emissions of volatile organic compounds in flowers and herbivory-elicited leaves.

Munawar et al., 2023, Current Biology *33*, 2321–2329
June 5, 2023
https://doi.org/10.1016/j.cub.2023.04.074

CellPress

Current Biology

CellPress

Report

Tissue-specific regulation of volatile emissions moves predators from flowers to attacked leaves

Asim Munawar,[1,7] Yi Xu,[2] Amr S. Abou El-Ela,[1,3] Yadong Zhang,[1] Jian Zhong,[1] Zhiyao Mao,[1] Xuan Chen,[1] Han Guo,[4] Chao Zhang,[1] Yiqiao Sun,[5] Zengrong Zhu,[1] Ian T. Baldwin,[6] and Wenwu Zhou[1,8,*]

[1]Ministry of Agricultural and Rural Affairs Key Laboratory of Molecular Biology of Crop Pathogens, Institute of Insect Science, Zhejiang University, Hangzhou 310058, China

[2]Department of Plant Pathology, Nanjing Agricultural University, Nanjing 210095, China

[3]Department of Plant Protection, Faculty of Agriculture (Saba Basha), Alexandria University, Alexandria 21531, Egypt

[4]Department of Economic Plants and Biotechnology, Yunnan Key Laboratory for Wild Plant Resources, Kunming Institute of Botany, Chinese Academy of Sciences, Kunming 650201, China

[5]Department of Environmental Systems Science, ETH Zurich, Universitätstrasse 6, 8006 Zurich, Switzerland

[6]Department of Molecular Ecology, Max Planck Institute for Chemical Ecology, Hans-Knöll-Str. 8, 07745 Jena, Germany

[7]Twitter: @AsimMunawar62

[8]Lead contact

*Correspondence: wenwuzhou@zju.edu.cn

https://doi.org/10.1016/j.cub.2023.04.074

SUMMARY

Plant-predator mutualisms have been widely described in nature.[1,2] How plants fine-tune their mutualistic interactions with the predators they recruit remains poorly understood. In the wild potato (*Solanum kurtzianum*), predatory mites, *Neoseiulus californicus*, are recruited to flowers of undamaged plants but rapidly move downward when the herbivorous mites, *Tetranychus urticae*, damage leaves. This "up-down" movement within the plant corresponds to the shift of *N. californicus* from palynivory to carnivory, as they change from feeding on pollen to herbivores when moving between different plant organs. This up-down movement of *N. californicus* is mediated by the organ-specific emissions of volatile organic compounds (VOCs) in flowers and herbivory-elicited leaves. Experiments with exogenous applications, biosynthetic inhibitors, and transient RNAi revealed that salicylic acid and jasmonic acid signaling in flowers and leaves mediates both the changes in VOC emissions and the up-down movement of *N. californicus*. This alternating communication between flowers and leaves mediated by organ-specific VOC emissions was also found in a cultivated variety of potato, suggesting the agronomic potential of using flowers as reservoirs of natural enemies in the control of potato pests.

RESULTS AND DISCUSSION

Mutualism, the association between two species in which each benefits, is a widespread phenomenon in nature.[3–5] Plant-natural enemy mutualisms have been widely described and are second only to plant-pollinator interactions.[6] Predators are among the most abundant and influential natural enemies, which can structure ecological communities.[7,8] When they interact, plants offer shelter, prey, and reliable information about prey location and feeding behavior and alternative food sources to predators, which reward these efforts by consuming herbivores.[9,10] Among the alternative food sources plants provide to predators, protein-rich pollen is particularly favored by many predator species when folivorous insects are rare.[10–12] The over-consumption of pollen by predators, however, may negatively affect the pollination of plants,[13] which creates a "dilemma" for the biological control of insect pests in crop systems where predators are released in large quantities.[14,15] Although it has been shown that plants can use diverse chemical cues to attract predators from the surrounding environment,[16–19] little is known about how plants fine-tune these mutualistic interactions so as to optimize the predation behavior of the recruited predators.

Predatory mites (PDMs) belong to a large group of well-known carnivorous invertebrates recruited by many plants in nature, where they function as reliable natural enemies preying on herbivores.[20–22] *N. californicus* is a PDM globally used in the biological control of crop pests.[23] Here, we show that it displays an up-down movement when recruited to wild potato, *S. kurtzianum* plants. When they first colonize plants, PDMs mainly move upward and congregate in flowers (Figure S1A); however, when plants are damaged by the herbivorous two-spotted spider mites, *Tetranychus urticae* (TSM), the predators rapidly (within 2 h) move downward to the attacked leaves (Figure 1A). It is well-recognized that many predator species visit flowers in nature, where they obtain additional dietary components.[24] To find out why PDMs move to flowers in control, TSM-unattacked plants, we dissected flowers to observed PDM behavior and discovered that they fed on pollen in flowers[25] (Figure 1B; Video S1). Apparently, this behavior is important for PDMs because without herbivorous prey, these mites do not survive on other plant tissues (Figure 1C), and pollen serves as a nourishing and

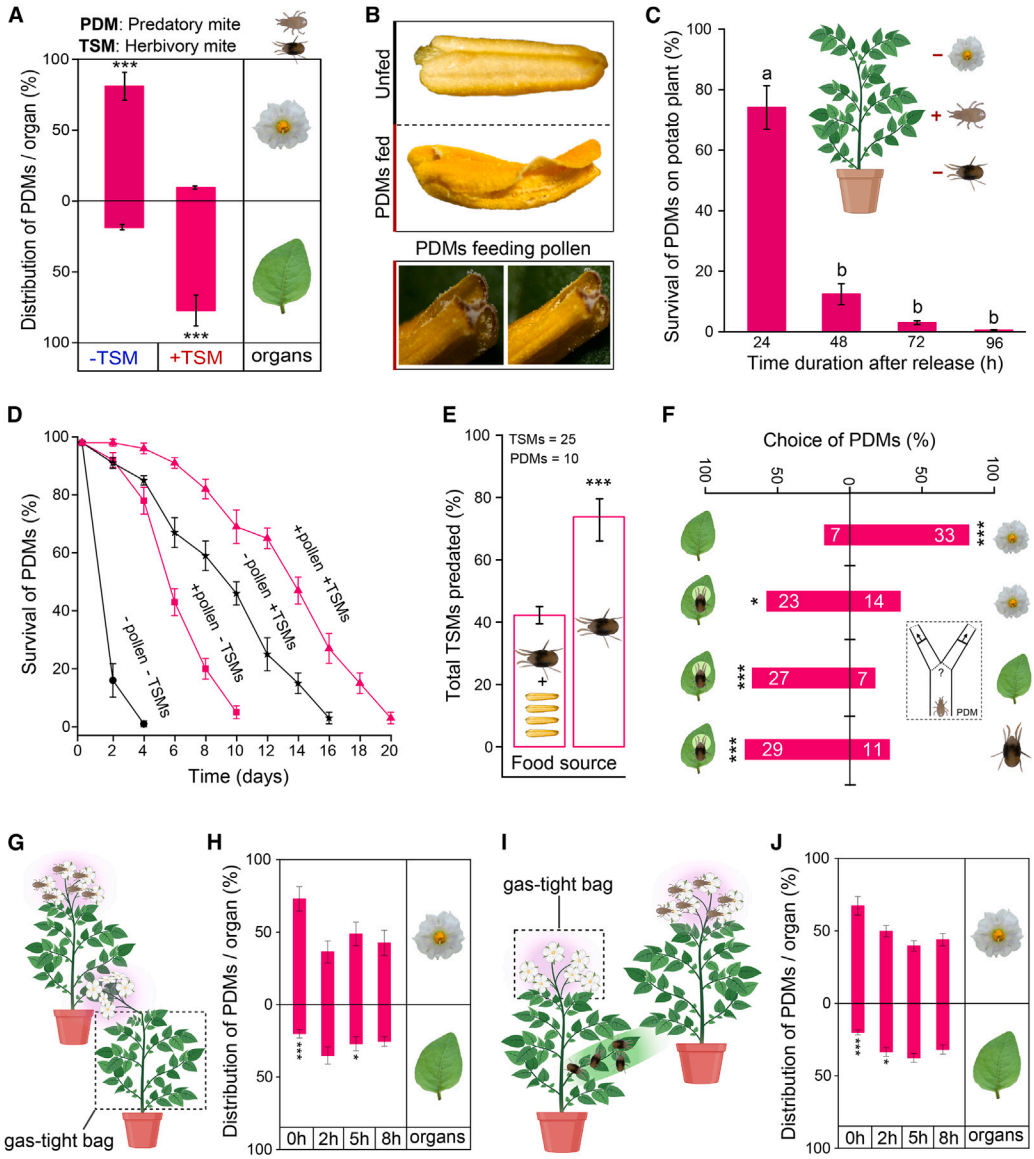

Figure 1. The up-down movement of *Neoseiulus californicus* and their preferences for and survival on different food and VOC sources

(A) The *N. californicus* (PDM) recruitment by different plant organs in the presence or absence of *T. urticae* (TSM) herbivorous mites. −TSMs, absence of TSMs on plants (n = 30 PDMs per plant, n = 5 flowers per plant, n = 7 plants); +TSMs, presence of TSMs on plants (n = 30 PDMs per plant, n = 100 TSMs per plant, n = 5 flowers per plant, n = 7 plants). Individual leaflets or flowers in the rectangular boxes represent the distribution of PDMs among plant organs.

(B) Typical image of anthers damaged by PDMs.

(C) PDM survival rate on plants lacking flowers and TSMs (n = 235 PDMs per plant; n = 5 plants).

(D) Survival of PDMs fed different food types (n = 20 PDMs, n = 30 TSMs, n = 30 anthers per replicate, n = 5 replicate for each group). Fresh anthers were provided as a pollen source.

(E) TSMs predated by PDMs. PDMs were offered TSMs alone or complemented with anthers (n = 10 replicates per group).

(F) The olfactory responses of PDMs to distinct plant organs in Y-tube olfactometer tests (n = 40 PDMs per test). A compound leaf infested with TSMs (n = 15 TSMs per leaflet) for 2 h was used as an induced leaf for choice tests.

(G) Manipulation of odor sources with additional flowers. The vegetative parts of the added plant were enclosed in a gas-tight bag.

(H) The PDM distribution among plant organs following flower-odors manipulations (n = 250 PDMs per plant, n = 10 plants per group).

(I) Manipulation of odor sources with the additional TSM-induced leaves. The compound leaves of 2 h TSM-infested plants (n = 15 TSMs per leaflet) were used as sources of induced odors. The flowers of the added plant were enclosed in a gas-tight bag.

(J) The PDMs distribution among plant organs following induced-leaf odors manipulations (n = 250 PDMs per plant, n = 10 plants per group).

Statistical analysis for (C) and (D) was conducted with one-way ANOVA followed by Tukey's post hoc tests. Letters indicate the significant difference among the treatment groups at $p \leq 0.05$. For (D), letters were not added to simplify the reading. The data were analyzed for (E) with a t test ($p \leq 0.05$); for (F) with Pearson's chi-squared tests (χ^2; $p \leq 0.05$); and for (A), (H), and (J), with generalized linear models (GLMs) by specifying Poisson errors. The asterisks indicate statistical differences in GLM tests (0 "***" 0.001 "**" 0.05 "*"). The data are mean ± SE.

See also Figure S1 and Video S1.

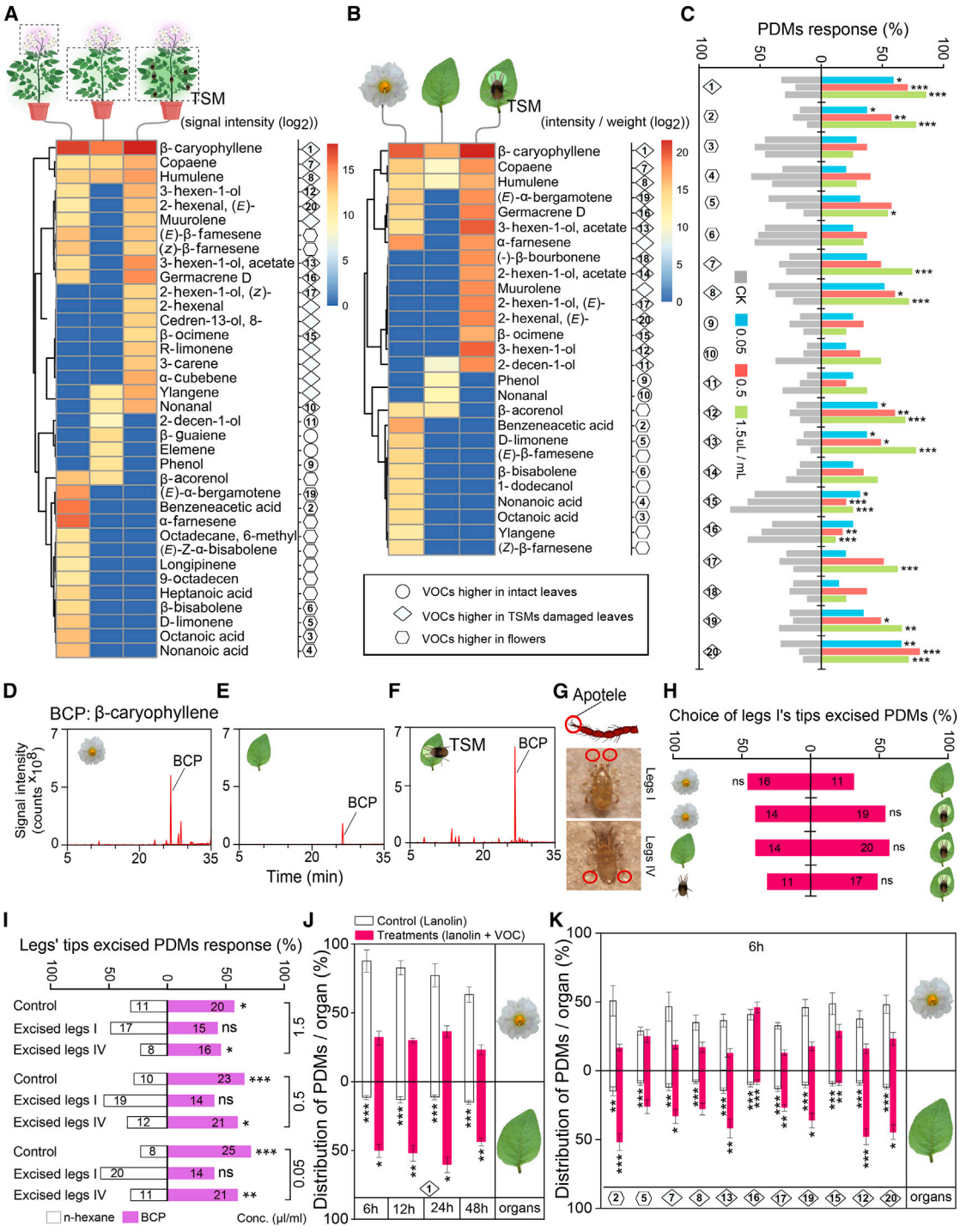

Figure 2. The organ-specific release of VOCs and their influence on *Neoseiulus californicus*'s olfactory behaviors

(A) Heatmap showing the intensities of a subset of VOCs from flowers, intact, or elicited plants trapped using Tenax-TA sorbent tubes (n = 6 plants per group). For floral VOCs trapping, every plant with uniform flowers (n = 5 flowers per plant) was used.[30] The color of each box represents the relative intensity of individual VOC. The dotted rectangular boxes on plants represent the bag used to enclose specific plant parts. For induced VOC trappings, the plants were infested with *T. urticae* (TSMs) (n = 300 per plant).

(B) Heatmap showing the intensities of a subset of VOCs from flowers, intact, or induced plants sampled with polydimethylsiloxane (PDMS) tubes (n = 7 flowers, n = 7 plants per group). Seven flowers pooled from individual plants were incubated separately with PDMS tubes in glass vials for floral VOC samplings. For elicited VOC samplings, the individual compound leaves from TSM-infested plants (n = 15 TSMs per leaflet) were incubated with PDMS tubes in a rectangular plastic box.

(legend continued on next page)

attractive food source[11] (Figures 1D and 1E). Moreover, although the movement of predators on plants is known to be influenced by different plant traits,[26–28] using Y-tube olfactometers, we found that PDMs showed a strong olfactory preference for different plant tissues in the following order: TSM-damaged leaves > flowers > intact leaves (Figure 1F). Interestingly, when the undamaged leaves were supplied with odor sources from flowers or TSM-damaged leaves (Figures 1G, 1I, and S1I), PDMs frequently moved downward to leaves from the flowers where they had gathered (Figures 1H, 1J, and S1J). Moreover, when flowers were supplied with odors from the TSM-attacked leaves (Figure S1K), PDM congregations in flowers were further enlarged (Figure S1L). From these results, we inferred that olfactory cues mediate the movement of PDMs between different plant parts. As PDMs did not show a preference for flowers from either TSM-attacked or unattacked plants (Figures S1B–S1D), their downward movement on TSM-damaged plants was more likely to result from a "pull" from attacked leaves than a "push" from flowers.

Plants synthesize and release a complex bouquet of volatile organic compounds (VOCs) that function as chemical cues guiding the movements of many animals interacting with plants.[18,29] It remains unclear how olfactory cues from flowers or leaves mediate the movement behavior of PDMs on *S. kurtzianum* plants. To identify the VOCs that might mediate the up-down movement of PDMs, we first analyzed the VOCs from three organs of *S. kurtzianum* plants—flowers, intact leaves, and TSM-attacked leaves, using both Tenax-TA trapping (for pooled samples of the same tissues) (Figures 2A, S2A, and S2B) and polydimethylsiloxane (PDMS) tube sampling (for individual tissue samples) (Figures 2B, 2D–2F, S2B, and S2C) methods. Commercially available synthetic versions of the identified VOCs were used to test PDMs' olfactory responses in Y-tube olfactometer choice assays (Figure 2C). Among the three organs studied, intact leaves emitted the fewest number of VOCs (Figures 2D–2F), and the two most abundant VOCs (phenol and nonanal) specifically emitted from undamaged leaves did not elicit PDMs' responses in the Y-tube assays (Figures 2A–2C). Flowers release several specific VOCs (benzeneacetic acid, octanoic acid, nonanoic acid, D-limonene, β-bisabolene, etc.) (Figures 2A and 2B), and among these, benzeneacetic acid was highly attractive to PDMs. Although many VOCs are co-emitted by both TSM-damaged leaves and flowers (β-caryophyllene, copaene, humulene, (*E*)-α-bergamotene, germacrene D, 3-hexen-1-ol acetate, etc.) (Figures 2A and 2B) and are strongly attractive to PDMs (except for germacrene D) (Figure 2C), most are emitted in higher amounts from TSM-attacked leaves. In addition, among the VOCs dominantly emitted in TSM-damaged leaves, three VOCs (3-hexen-1-ol, 2-hexen-1-ol, (*E*)-, 2-hexenal, (*E*)-) attracted PDMs, three (2-decen-1-ol, (−)-β-bourbonene, 2-hexen-1-ol acetate) did not influence PDMs movement in Y-tubes, and only one (β-ocimene) repelled PDMs (Figures 2B and 2C).

It is well-documented that PDMs sense plant VOCs by olfactory sensilla that reside in a dorsal field at the tip of their first pair of legs.[31] When these leg tips (apotele) are excised, the speed of mite movements is unaffected, and they move freely in Y-tube olfactometers (Figures S3A–S3F). To discover how the bioactive VOCs identified above regulate PDMs' up-down movement, we conducted the olfactory choice assays with these tip-excised PDMs and with PDMs that had their fourth leg-tips ablated, as ablation controls. Removal of the first leg-tips interrupted PDMs' olfactory preference for both synthetic β-caryophyllene and VOCs from plant organs (Figures 2G–2I), consistent with the inference that olfaction plays a crucial role in mediating their up-down movement behavior. To evaluate if the 12 bioactive VOCs, namely those showing attraction/repellence response to PDMs (Figure 2C), can mediate the distribution of PDMs among different plant organs, we released PDMs to plants 4 h after these VOCs were applied to intact leaves and observed how the PDMs distributed themselves on the VOC-treated plants. All 10 attractive VOCs (β-caryophyllene, benzeneacetic acid, D-limonene, copaene, humulene, 3-hexen-1-ol acetate, 2-hexen-1-ol, (*E*)-, (*E*)-α-bergamotene, 3-hexen-1-ol, 2-hexenal, (*E*)-) disrupted the congregation of PDMs in flowers, whereas the 2 repellant VOCs (germacrene D and β-ocimene) did not influence PDM distributions between the two organs (Figures S2J and 2K). In summary, the organ-specific VOC emissions correlated strongly with the up-down movement behavior of the PDMs on plants, and their preferences in Y-tube bioassays.

Plants use sophisticated signaling systems to optimize their allocations of limited photosynthetic products and minimize the costs of accumulating and releasing specialized metabolites, including VOCs.[32] Although phytohormones are well-recognized as key signals in regulating the production and emission of VOCs,[33] it remains unclear how phytohormonal signaling

(C) The olfactory response of *N. californicus* (PDM) to synthetic plant VOCs standards in Y-tube olfactometer tests (n = 35 PDMs per test). The right panel bars display PDM responses to different concentrations of VOCs, while the left panel's gray bars display PDM responses to n-hexane (control).
(D–F) Thermal desorption-mass spectrometry-gas chromatography (TD-GC-MS) total ion chromatograms (TICs) of VOCs released by different organs of the *S. kurtzianum* plant. B-caryophyllene (BCP), the dominant VOC released by flowers and leaves, was trapped.
(G) Red circles on leg illustrations demark the terminal apotele (first or fourth) that were excised under a microscope.
(H) The olfactory responses to PDMs-trapped VOCs from different plant organs of foreleg-excised PDMs in Y-tube olfactometer tests (n = 35 PDMs per test).
(I) The olfactory responses of foreleg-excised PDMs to synthetic BCP (n = 35 PDMs per test). n-hexane was used as a control.
(J) The application of synthetic BCP to intact leaves and distribution of PDMs among plant organs at different time intervals (n = 235 PDMs per plant, n = 4 plants per group).
(K) The application of other synthetic VOCs to intact leaves and distribution of PDMs among plant organs (n = 235 PDMs per plant, n = 7 plants per group). VOCs used in the following tests were selected based on PDM responses in Y-tube olfactometers.
For (A) and (B), the data were log-transformed to meet the assumptions of normality. Hierarchical cluster analysis using Euclidean distances and the Ward variance method was used to plot "heatmaps" in R. For (C), (G), and (I), the response data were analyzed by Pearsons chi-squared tests (χ^2; $p \leq 0.05$). Statistical analysis for (J) and (K) used a GLM model by specifying Poisson errors. The asterisks indicate statistical differences among the individual groups tested (0 "***" 0.001 "**" 0.05 "*"). The data are mean ± SE.
See also Figures S2 and S3.

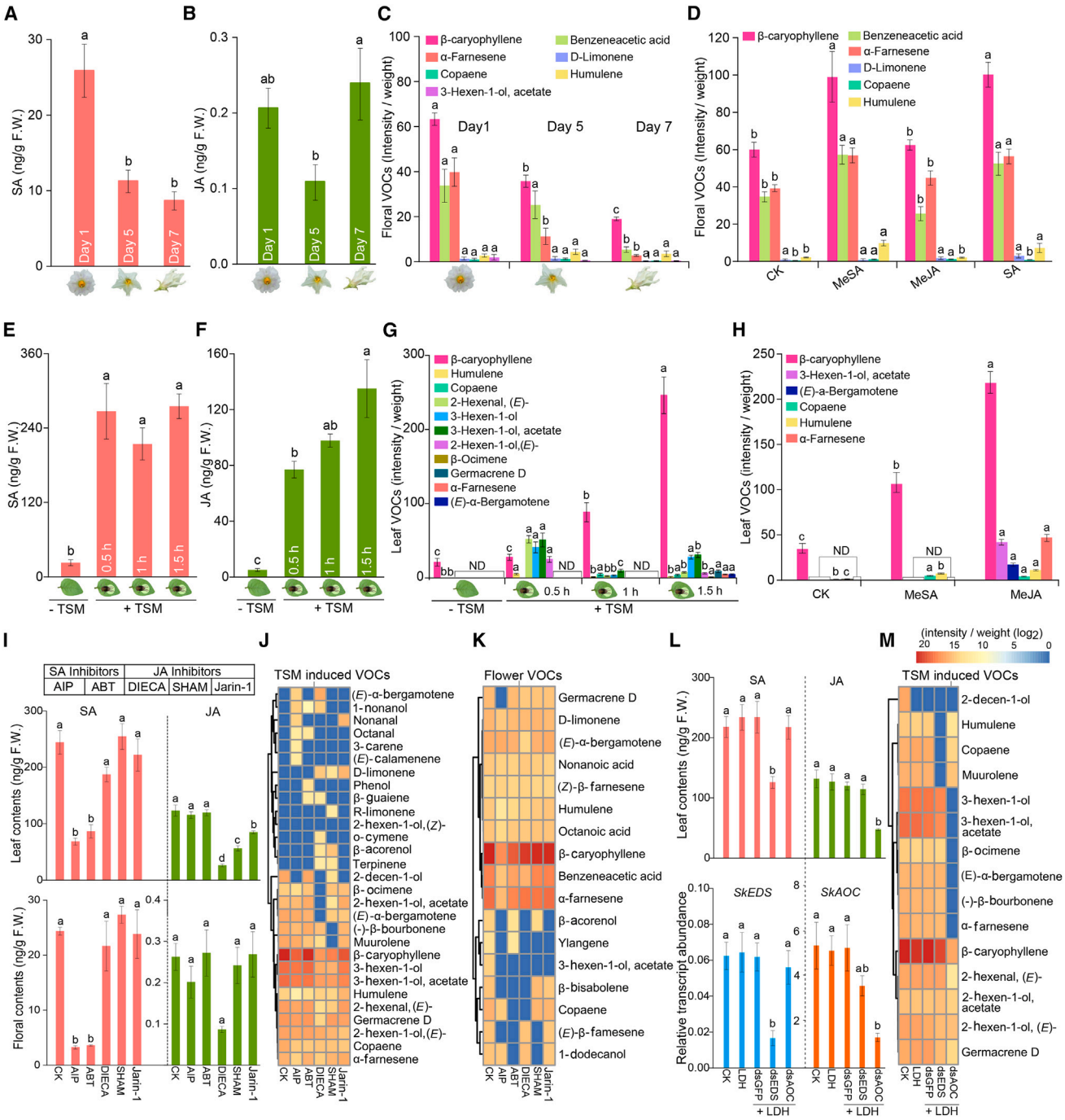

Figure 3. The spatiotemporal regulation of VOCs emission is mediated by phytohormones

(A–C) The pooled phytohormone contents (from different aged flowers) and floral VOCs released (n = 3–4 flowers per replicate, n = 7 plants per group). Individual flowers pooled from different plants were incubated with PDMS in glass vials. The displayed VOCs were selected based on their dominance in floral bouquets.

(D) Elicitors were applied to floral pedicels to elicit release of floral VOCs that were trapped on PDMS tubes (n = 7 plants per group).

(E and F) Phytohormone contents in pooled leaves at different time intervals after TSM infestation (n = 7 plants per group).

(G) Similarly, the amounts of VOCs released from leaves following TSM infestations (n = 7 plants per group). The displayed VOCs were selected based on their dominance in leaf headspace.

(H) Leaf VOCs released from plants whose leaves had been treated with different elicitors (n = 5 plants per group).

(I) Phytohormone contents in leaves or flowers sprayed with different chemical inhibitors (n = 8 plants per group) for SA (1-aminobenzotriazole [ABT]; 2-aminoindane-2-phosphonic acid [AIP]) and JA (sodium diethyldithiocarbamate [DIECA]; salicylhydroxamic acid [SHAM]; jasmonic acid-amido synthetase [Jarin-1]); distilled water containing 0.02% (vol/vol) Tween 20 and 0.01% ethanol was applied as a control treatment (CK).

(legend continued on next page)

mediates the differential emission of VOCs and the resulting PDM movement behavior. To answer this question, we first analyzed the concentrations of two key phytohormones, jasmonic acid (JA) and salicylic acid (SA), in the three organs—flowers, intact leaves, and TSM-damaged leaves. Although only SA accumulated to high levels in flowers (Figures 3A and 3B), the levels of both JA and SA were elevated in TSM-damaged leaves (Figures 3E and 3F). Among the VOCs that attract or repel PDMs, the two dominant floral VOCs (β-caryophyllene and benzeneacetic acid) showed an emission pattern similar to the levels of SA in this organ (Figures 3A and 3C), and the three dominant VOCs released from TSM-damaged leaves (β-caryophyllene, 3-hexen-1-ol, 3-hexen-1-ol acetate) tracked the levels of JA and SA in this organ (Figure 3G). To further evaluate how SA or JA signaling regulates the emission of these VOCs, we supplied flowers with methyl salicylate (MeSA), methyl jasmonate (MeJA), and SA and treated leaves with MeSA and MeJA. The emissions of the dominant floral VOCs (β-caryophyllene, benzeneacetic acid, and α-farnesene) were elicited by enhanced SA signaling (Figure 3D); in leaves, although the release of β-caryophyllene, copaene, and humulene could be elicited by both SA and JA signaling, 3-hexen-1-ol acetate, α-farnesene, and (*E*)-α-bergamotene could be induced only by enhancing JA-signaling (Figure 3H). Interestingly, when MeJA-treated leaves were placed next to intact leaves, the PDMs on the undamaged plants were "pulled-down" from the flowers to the leaves; however, when MeSA-treated leaves were placed next to the intact leaves, no such effect was observed (Figures S1M–S1P), indicating that SA and JA signaling play different roles in regulating these VOC emissions in leaves.

To further examine the roles of these phytohormones in the release of VOCs, we applied the biosynthetic inhibitors for SA (1-aminobenzotriazole [ABT]; 2-aminoindane-2-phosphonic acid [AIP]) and JA (sodium diethyldithiocarbamate [DIECA]; salicylhydroxamic acid [SHAM]; JA-amido synthetase [Jarin-1]) to leaves and flowers.[34–37] AIP or ABT treatments reduced SA accumulations in leaves and flowers, whereas DIECA, SHAM, and Jarin-1 treatments reduced JA accumulations in leaves (Figure 3I). Meanwhile, these inhibitors also influenced VOC emissions in TSM-attacked leaves (β-caryophyllene, 3-hexen-1-ol, 3-hexen-1-ol acetate) or flowers (β-caryophyllene, benzeneacetic acid, and α-farnesene) (Figures 3J and 3K). Moreover, to further probe the role of phytohormonal regulation of VOC emissions in leaves, we silenced key biosynthetic genes for SA (*SkEDS1*) and JA (*SkAOC*) by the topical application of their -double-stranded RNAs (dsRNAs) loaded onto layered double hydroxide (LDH) clay (BioClay) nanosheets[38,39] (Figures S4A–S4H). Spraying leaves with a loading ratio of 1:6 dsRNA-LDH reduced both the SA and JA contents and the transcript abundances of their biosynthetic genes, *SkEDS1* and *SkAOC*, respectively (Figure 3L). Moreover, VOC emissions were predictably changed following dsRNA-LDH complexes applications: 3 VOCs (humulene, copaene, and muurolene) were decreased in *SkEDS1*-silenced plants, whereas 6 (3-hexen-1-ol, 3-hexen-1-ol acetate, β-ocimene, (*E*)-α-bergamotene, and (−)-β-bourbonene) were decreased in *SkAOC*-silenced plants. Furthermore, the β-caryophyllene emission was strongly reduced in *SkAOC*-silenced plants, as compared with *SkEDS1*-silenced, GFP-dsRNA, LDH only, and CK-treated plants (Figure 3M). Additionally, the number of TSM feeding spots on *SkAOC*- and *SkEDS1*-silenced plants and PDM predation on *SkAOC*-silenced plants were higher compared with those of controls (Figures S4I–S4K). From these results, we conclude that the differential accumulation of phytohormones is responsible for the tissue-specific emission of VOCs in *S. kurtzianum*.

We further examined the behavioral responses of PDMs for plants sprayed with the chemical inhibitors or dsRNA-LDH. The application of SA inhibitors (AIP and ABT) on flowers and JA inhibitors (DIECA, SHAM, and Jarin-1) on leaves significantly disrupted the PDMs' congregation behavior among plant organs (Figures 4A and 4B). Likewise, the PDM gatherings on TSM-damaged leaves were changed at days 10 and 20 post AOC-dsRNA leaf spray, whereas the PDMs distribution remained unchanged by the applications of EDS1-dsRNA, GFP-dsRNA, LDH only, and CK to leaves (Figures 4C and 4D). Moreover, the LDH alone did not alter the behavioral response of PDMs (Figures S4L–S4P). These results are consistent with the inference that differential phytohormonal signaling mediates the up-down gathering behavior of the PDMs.

In conclusion, PDMs, on the wild potato *S. kurtzianum* plants, change their feeding behavior from palynivory to carnivory, as they move from flowers to herbivore-attacked leaves. We tested the hypotheses that this up-down movement of PDMs was mediated by (1) plant responses induced by TSM herbivory, (2) by constitutive (floral) and induced (TSM-attacked leaves) bioactive VOCs, and (3) differences in floral and leaf JA and SA signaling. Constitutive accumulations of SA in flowers promote the emissions of bioactive VOCs that facilitate the congregation of PDMs in flowers where they feed on pollen in the absence of the TSM prey. When TSMs attack leaves, interactions of JA and SA signaling elicit the emission of bioactive VOCs (herbivore-induced plant volatiles [HIPVs]) that attract PDMs from their floral congregation sites to attacked leaves, where they prey on TSMs (Figure 4E). Thus, this organ-specific VOC regulation mediates an herbivory-inducible communication system between flowers and leaves for a predatory Arachnida in a wild potato

(J and K) Heatmaps depicting relative amounts of a subset of VOCs released from flowers and TSM-damaged leaves following inhibitors applications (n = 7 plants per group).

(L) Phytohormone contents and transcript abundances of related genes (*SkAOC*, *SkEDS*) in leaves sprayed with layered double hydroxide (LDH) clay nanosheets mixed with different compounds (n = 6 plants per group). The dsRNAs of selected genes (dsAOC for *SkAOC*, dsEDS for *SkEDS*) were loaded on LDH for topical delivery. The control plants were sprayed with water (CK) or LDH only (LDH) or dsRNA-LDH for green fluorescent protein (dsGFP).

(M) The heatmap showing the intensities of a subset of VOCs from TSM-damaged leaves following the dsRNA-LDH application (n = 6 plants per group).

Statistical analyses were conducted with one-way ANOVAs followed by Tukey's post hoc tests. Letters indicate significant differences among treatment groups at $p \leq 0.05$. The VOC data were log-transformed to meet the assumptions of normality. Hierarchical cluster analysis using Euclidean distances and the Ward variance method were used to plot heatmaps in R. The data are presented as mean ± SE.

See also Figures S1 and S4.

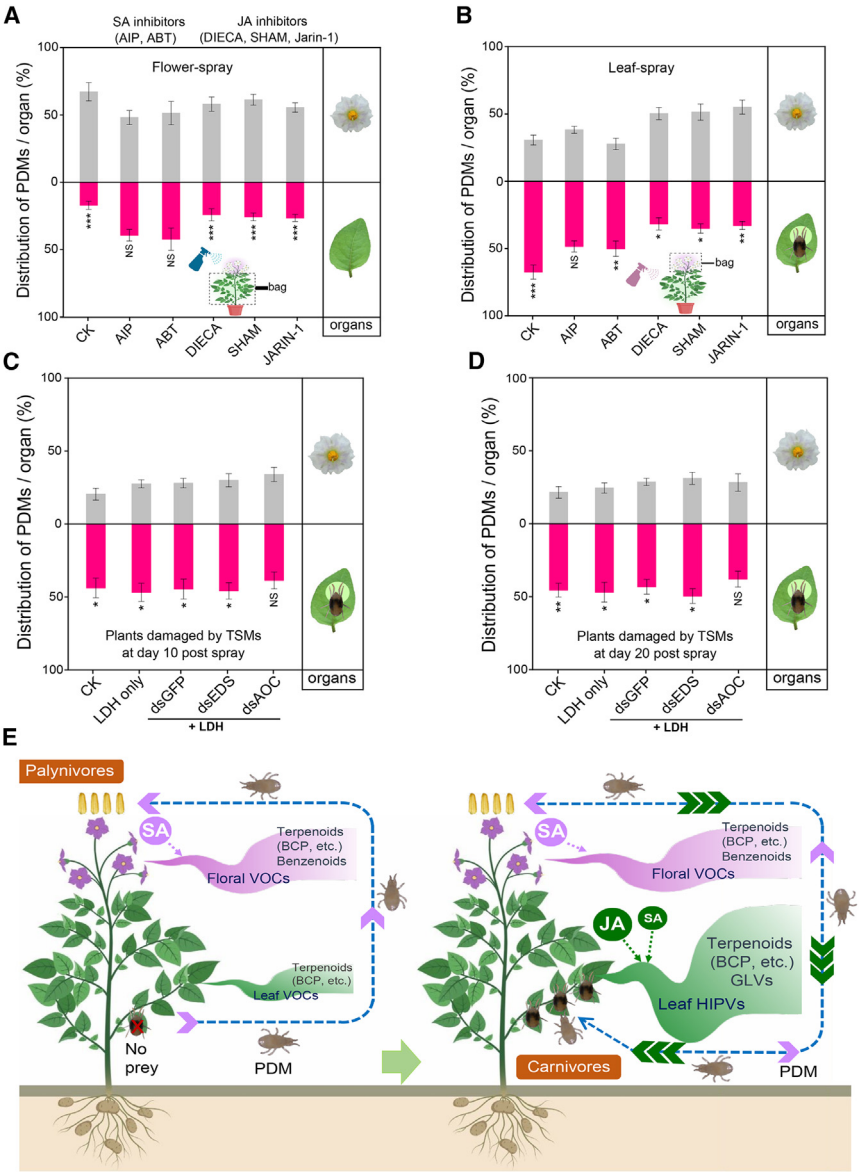

Figure 4. Suppressing phytohormone signaling influences the intra-plant movement of *Neoseiulus californicus*

(A) *N. californicus* (PDM) distributions on plants whose flowers were pretreated with different chemical inhibitors (n = 7 plants per treatment group) for SA (1-aminobenzotriazole [ABT]; 2-aminoindane-2-phosphonic acid [AIP]) and JA (sodium diethyldithiocarbamate [DIECA]; salicylhydroxamic acid [SHAM]; jasmonic acid-amido synthetase [Jarin-1]); distilled water containing 0.02% (vol/vol) Tween 20 and 0.01% ethanol was applied as a control treatment (CK). The dotted rectangular box represents the bag used to enclose plant parts during applications of inhibitors to avoid cross-contamination.

(B) The PDM distribution on the plants whose leaves were pretreated with different chemical inhibitors (n = 7 plants per treatment group).

(C and D) The distribution of PDMs on plants whose leaves had been sprayed with layered double hydroxide (LDH) clay nanosheets mixed with different compounds for 10 or 20 days (n = 7 plants per treatment group). The dsRNAs of selected genes (dsAOC for *SkAOC*, dsEDS for *SkEDS*) were loaded on LDH for topical delivery. Control plants were sprayed with water (CK) or LDH only (LDH), or dsRNA-LDH for green fluorescent protein (dsGFP).

(E) A graphical illustration of the central findings of this study.

Statistical analyses were conducted using GLMs by specifying Poisson errors. The asterisks indicate statistical differences in GLM tests (0 "***" 0.001 "**" 0.05 "*"). The data are presented as mean ± SE. NS, not significant.

See also Figure S4.

whose reproduction is achieved through both seeds and tubers.[40]

Previous research had established that herbivory-induced responses can antagonize the attraction of pollinators[41] and the evolution of pollinator-attracting floral traits.[42] Here, we demonstrate a synergy between HIPVs and constitutively produced floral volatiles; the floral volatiles, which presumably are important in attracting pollinators, are also important in attracting PDMs and allow flowers to become reservoirs of natural enemies that are subsequently recruited to attacked leaves by HIPVs. As similar up-down responses were also identified in a commonly used potato cultivar (c.v. Lishu 6) (Figures S1E–S1H), future research into the mechanisms of how phytohormones regulate this organ-specific VOC release could facilitate its integration into biological control of agricultural pests. In potato-cropping systems, flowers could function as important reservoirs of natural enemies, which by the signaling system described here could be mobilized for the effective control of folivorous pests and minimize the reproduction cost resulting from the pollen-feeding behavior of beneficial predators. Given that *N. californicus* and *S. kurtzianum* both originated from South America,[43,44] it would also be interesting to evaluate if this up-down behavioral regulation improves the fitness of both organisms and hence could be considered a true mutualistic interaction.

STAR★METHODS

Detailed methods are provided in the online version of this paper and include the following:

- KEY RESOURCES TABLE
- RESOURCE AVAILABILITY
  - Lead contact
  - Materials availability
  - Data and code availability
- EXPERIMENTAL MODEL AND SUBJECT DETAILS
  - Chemicals
  - Experimental plants and organisms

SUPPLEMENTAL INFORMATION

Supplemental information can be found online at https://doi.org/10.1016/j.cub.2023.04.074.

ACKNOWLEDGMENTS

This work was funded by the National Nature Science Foundation of China (grant no. 32272636 and 32072432) and the Key Research and Development Program of Zhejiang Province (grant no. 2019C04007). The supporting agency had no directive in data collection, research designs, data analysis, manuscript preparation, or publishing decisions. We appreciate Dr. Bizeng Mao for her help with the potato tissue culture, and Dr. Lijuan Mao for her help with the chemical analysis.

AUTHOR CONTRIBUTIONS

Conceptualization, W.Z., I.T.B., and A.M.; methodology, A.M., W.Z., Y.X., A.S.A.E.-E., Y.Z., J.Z., Z.M., X.C., H.G., C.Z., Y.S., and Z.Z.; investigation, A.M., W.Z., A.S.A.E.-E., Y.Z., J.Z., Z.M., X.C., H.G., C.Z., and Y.S.; writing – original draft, A.M. and W.Z.; writing – review and editing, W.Z., I.T.B., H.G., and Y.X.; funding acquisition, W.Z. and Z.Z.; resources, W.Z. and Y.X.; supervision, W.Z.

DECLARATION OF INTERESTS

The authors declare no competing interests.

INCLUSION AND DIVERSITY

We support inclusive, diverse, and equitable conduct of research.

Received: March 27, 2023
Revised: April 26, 2023
Accepted: April 28, 2023
Published: May 23, 2023

REFERENCES

1. Meehan, C.J., Olson, E.J., Reudink, M.W., Kyser, T.K., and Curry, R.L. (2009). Herbivory in a spider through exploitation of an ant-plant mutualism. Curr. Biol. *19*, R892–R893.
2. Benoit, A.D., and Kalisz, S. (2020). Predator effects on plant-pollinator interactions, plant reproduction, mating systems, and evolution. Annu. Rev. Ecol. Evol. Syst. *51*, 319–340.
3. Bronstein, J.L., Alarcón, R., and Geber, M. (2006). The evolution of plant–insect mutualisms. New Phytol. *172*, 412–428.
4. Krupa, J.J., Hopper, K.R., Gruber, S.B., Schmidt, J.M., and Harwood, J.D. (2020). Plant-animal interactions between carnivorous plants, sheet-web spiders, and ground-running spiders as guild predators in a wet meadow community. Ecol. Evol. *10*, 4762–4772.
5. Inbar, M., and Gerling, D. (2008). Plant-mediated interactions between whiteflies, herbivores, and natural enemies. Annu. Rev. Entomol. *53*, 431–448.
6. Bascompte, J. (2019). Mutualism and biodiversity. Curr. Biol. *29*, R467–R470.
7. Takabayashi, J., and Dicke, M. (1996). Plant—carnivore mutualism through herbivore-induced carnivore attractants. Trends Plant Sci. *1*, 109–113.
8. Mappes, J., Kokko, H., Ojala, K., and Lindström, L. (2014). Seasonal changes in predator community switch the direction of selection for prey defences. Nat. Commun. *5*, 5016.
9. Messelink, G.J., Bennison, J., Alomar, O., Ingegno, B.L., Tavella, L., Shipp, L., Palevsky, E., and Wäckers, F.L. (2014). Approaches to conserving natural enemy populations in greenhouse crops: current methods and future prospects. BioControl *59*, 377–393.
10. Jacometti, M., Jørgensen, N., and Wratten, S. (2010). Enhancing biological control by an omnivorous lacewing: floral resources reduce aphid numbers at low aphid densities. Biol. Control *55*, 159–165.
11. Samaras, K., Pappas, M.L., Pekas, A., Wäckers, F., and Broufas, G.D. (2021). Benefits of a balanced diet? Mixing prey with pollen is advantageous for the phytoseiid predator *Amblydromalus limonicus*. Biol. Control *155*, 104531.
12. Villa, M., Somavilla, I., Santos, S.A.P., Lopez-Saez, J.A., and Pereira, J.A. (2019). Pollen feeding habits of *Chrysoperla carnea* adults in the olive grove agroecosystem. Agric. Ecol. Environ. *283*, 106573.
13. Telles, F.J., Gonzálvez, F.G., Rodríguez-Gironés, M.A., and Freitas, L. (2019). The effect of a flower-dwelling predator on a specialized pollination system. Biol. J. Linn. Soc. *126*, 521–532.
14. Li, D.F., Yan, X.C., Lin, Y., Wang, L., and Wang, Q. (2021). Do flowers removed of either nectar or pollen attract fewer bumblebee pollinators? An experimental test in *Impatiens oxyanthera*. AoB Plants *13*, plab029.
15. Abbott, K.R. (2010). Background evolution in camouflage systems: a predator–prey/pollinator-flower game. J. Theor. Biol. *262*, 662–678.
16. Cortés, L.E., Weldegergis, B.T., Boccalandro, H.E., Dicke, M., and Ballaré, C.L. (2016). Trading direct for indirect defense? Phytochrome B inactivation in tomato attenuates direct anti-herbivore defenses whilst enhancing volatile-mediated attraction of predators. New Phytol. *212*, 1057–1071.
17. Ye, M., Veyrat, N., Xu, H., Hu, L., Turlings, T.C.J., and Erb, M. (2018). An herbivore-induced plant volatile reduces parasitoid attraction by changing the smell of caterpillars. Sci. Adv. *4*, eaar4767.
18. Allmann, S., and Baldwin, I.T. (2010). Insects betray themselves in nature to predators by rapid isomerization of green leaf volatiles. Science *329*, 1075–1078.
19. Simpson, M., Gurr, G.M., Simmons, A.T., Wratten, S.D., James, D.G., Leeson, G., Nicol, H.I., and Orre-Gordon, G.U.S. (2011). Attract and reward: combining chemical ecology and habitat manipulation to enhance biological control in field crops. J. Appl. Ecol. *48*, 580–590.
20. Togashi, K., Goto, M., Rim, H., Hattori, S., Ozawa, R., and Arimura, G.I. (2019). Mint companion plants attract the predatory mite *Phytoseiulus persimilis*. Sci. Rep. *9*, 1704.
21. Hewitt, L.C., Shipp, L., Buitenhuis, R., and Scott-Dupree, C. (2015). Seasonal climatic variations influence the efficacy of predatory mites used for control of western flower thrips in greenhouse ornamental crops. Exp. Appl. Acarol. *65*, 435–450.
22. McMurtry, J.A., and Croft, B.A. (1997). Life-styles of phytoseiid mites and their roles in biological control. Annu. Rev. Entomol. *42*, 291–321.
23. Vacacela Ajila, H.E., Colares, F., Lemos, F., Marques, P.H., Franklin, E.C., Santos do Vale, W., Oliveira, E.E., Venzon, M., and Pallini, A. (2019).

Supplementary food for *Neoseiulus californicus* boosts biological control of *Tetranychus urticae* on strawberry. Pest Manag. Sci. *75*, 1986–1992.

24. He, X., Kiær, L.P., Jensen, P.M., and Sigsgaard, L. (2021). The effect of floral resources on predator longevity and fecundity: a systematic review and meta-analysis. Biol. Control *153*, 104476.
25. Eini, N., Jafari, S., Fathipour, Y., and Zalucki, M.P. (2022). How pollen grains of 23 plant species affect performance of the predatory mite *Neoseiulus californicus*. BioControl *67*, 173–187.
26. Agrawal, A.A. (2001). Phenotypic plasticity in the interactions and evolution of species. Science *294*, 321–326.
27. Koski, T.M., Lindstedt, C., Klemola, T., Troscianko, J., Mäntylä, E., Tyystjärvi, E., Stevens, M., Helander, M., and Laaksonen, T. (2017). Insect herbivory may cause changes in the visual properties of leaves and affect the camouflage of herbivores to avian predators. Behav. Ecol. Sociobiol. *71*, 97.
28. Ashra, H., and Nair, S. (2022). Review: trait plasticity during plant-insect interactions: from molecular mechanisms to impact on community dynamics. Plant Sci. *317*, 111188.
29. Pichersky, E., Noel, J.P., and Dudareva, N. (2006). Biosynthesis of plant volatiles: nature's diversity and ingenuity. Science *311*, 808–811.
30. Guo, H., Lackus, N.D., Köllner, T.G., Li, R., Bing, J., Wang, Y., Baldwin, I.T., and Xu, S. (2020). Evolution of a novel and adaptive floral scent in wild tobacco. Mol. Biol. Evol. *37*, 1090–1099.
31. Van Wijk, M., Wadman, W.J., and Sabelis, M.W. (2006). Morphology of the olfactory system in the predatory mite *Phytoseiulus persimilis*. Exp. Appl. Acarol. *40*, 217–229.
32. Koricheva, J., Barton, K.E., Iason, G.R., Dicke, M., and Hartley, S.E. (2012). The Ecology of Plant Secondary Metabolites: From Genes to Global Processes Ecological Reviews (Cambridge University Press), pp. 34–55.
33. Wei, J., van Loon, J.J.A., Gols, R., Menzel, T.R., Li, N., Kang, L., and Dicke, M. (2014). Reciprocal crosstalk between jasmonate and salicylate defence-signalling pathways modulates plant volatile emission and herbivore host-selection behaviour. J. Exp. Bot. *65*, 3289–3298.
34. Wang, Y., Wen, T., Huang, Y., Guan, Y., and Hu, J. (2018). Salicylic acid biosynthesis inhibitors increase chilling injury to maize (*Zea mays* L.) seedlings. Plant Growth Regul. *86*, 11–21.
35. Meesters, C., Mönig, T., Oeljeklaus, J., Krahn, D., Westfall, C.S., Hause, B., Jez, J.M., Kaiser, M., and Kombrink, E. (2014). A chemical inhibitor of jasmonate signaling targets JAR1 in *Arabidopsis thaliana*. Nat. Chem. Biol. *10*, 830–836.
36. Li, Y., Qiu, L., Zhang, Q., Zhuansun, X., Li, H., Chen, X., Krugman, T., Sun, Q., and Xie, C. (2020). Exogenous sodium diethyldithiocarbamate, a jasmonic acid biosynthesis inhibitor, induced resistance to powdery mildew in wheat. Plant Direct *4*, e00212.
37. Xin, Z., Zhang, Z., Chen, Z., and Sun, X. (2014). Salicylhydroxamic acid (SHAM) negatively mediates tea herbivore-induced direct and indirect defense against the tea geometrid *Ectropis obliqua*. J. Plant Res. *127*, 565–572.
38. Mitter, N., Worrall, E.A., Robinson, K.E., Li, P., Jain, R.G., Taochy, C., Fletcher, S.J., Carroll, B.J., Lu, G.Q., and Xu, Z.P. (2017). Clay nanosheets for topical delivery of RNAi for sustained protection against plant viruses. Nat. Plants *3*, 16207.
39. Yong, J., Zhang, R., Bi, S., Li, P., Sun, L., Mitter, N., Carroll, B.J., and Xu, Z.P. (2021). Sheet-like clay nanoparticles deliver RNA into developing pollen to efficiently silence a target gene. Plant Physiol. *187*, 886–899.
40. Camadro, E.L., Erazzú, L.E., Maune, J.F., and Bedogni, M.C. (2012). A genetic approach to the species problem in wild potato. Plant Biol. (Stuttg) *14*, 543–554.
41. Kessler, A., Halitschke, R., and Poveda, K. (2011). Herbivory-mediated pollinator limitation: negative impacts of induced volatiles on plant-pollinator interactions. Ecology *92*, 1769–1780.
42. Ramos, S.E., and Schiestl, F.P. (2019). Rapid plant evolution driven by the interaction of pollination and herbivory. Science *364*, 193–196.
43. De Moraes, G.J., McMurtry, J.A., Denmark, H.A., and Campos, C.B. (2004). A revised catalog of the mite family Phytoseiidae. Zootaxa *434*, 1–494.
44. Hardigan, M.A., Laimbeer, F.P.E., Newton, L., Crisovan, E., Hamilton, J.P., Vaillancourt, B., Wiegert-Rininger, K., Wood, J.C., Douches, D.S., Farré, E.M., et al. (2017). Genome diversity of tuber-bearing Solanum uncovers complex evolutionary history and targets of domestication in the cultivated potato. Proc. Natl. Acad. Sci. USA *114*, E9999–E10008.
45. Kabak, B., Karanfilci, M., Ersöz, T., and Kabak, M. (2016). Analysis of sports injuries related with shooting. J. Sports Med. Phys. Fitness *56*, 737–743.
46. Alkarkhi, A.F.M., Alqaraghuli, W.A.A., Alkarkhi, A.F.M., and Alqaraghuli, W.A.A. (2020). R statistical software. Applied Statistics for Environmental Science with R (Elsevier), pp. 11–27.
47. Munawar, A., Zhang, Y., Zhong, J., Ge, Y., Abou El-Ela, A.S., Mao, Z., Ntiri, E.S., Mao, L.J., Zhu, Z., and Zhou, W. (2022). Heat stress affects potato's volatile emissions that mediate agronomically important trophic interactions. Plant Cell Environ. *45*, 3036–3051.
48. Perkel, J.M. (2020). The software that powers scientific illustration. Nature *582*, 137–138.
49. Bohoussou, Y.N.D., Kou, Y.H., Yu, W.B., Lin, B., Bohoussou, Y.N., Kou, Y.H., Yu, W.B., Lin, B.J., Virk, A.L., Zhao, X., Dang, Y.P., and Zhang, H.L. (2022). Impacts of the components of conservation agriculture on soil organic carbon and total nitrogen storage: a global meta-analysis. Sci. Total Environ. *842*, 156822.
50. Minatani, K. (2015). Proposal for svg2dot an interoperable tactile graphics creation system using svg outputs from inkscape. Stud. Health Technol. Inform. *217*, 506–511.
51. Botti, J.M.C., Franzin, M.L., Fadini, M.A.M., and Melo, J.O.F. (2019). Preference of *Neoseiulus californicus* (Acari: Phytoseiidae) for volatiles of Bt maize induced by multiple herbivory. Rev. Bras. Entomol. *63*, 283–289.
52. Stewart-Jones, A., and Poppy, G.M. (2006). Comparison of glass vessels and plastic bags for enclosing living plant parts for headspace analysis. J. Chem. Ecol. *32*, 845–864.
53. Kallenbach, M., Oh, Y., Eilers, E.J., Veit, D., Baldwin, I.T., and Schuman, M.C. (2014). A robust, simple, high-throughput technique for time-resolved plant volatile analysis in field experiments. Plant J. *78*, 1060–1072.
54. Schuman, M.C., Barthel, K., and Baldwin, I.T. (2012). Herbivory-induced volatiles function as defenses increasing fitness of the native plant *Nicotiana attenuata* in nature. eLife *1*, e00007.
55. Baldwin, I.T., Schmelz, E.A., and Zhang, Z.P. (1996). Effects of octadecanoid metabolites and inhibitors on induced nicotine accumulation in *Nicotiana sylvestris*. J. Chem. Ecol. *22*, 61–74.
56. Wu, J., Hettenhausen, C., Meldau, S., and Baldwin, I.T. (2007). Herbivory rapidly activates mapk signaling in attacked and unattacked leaf regions but not between leaves of *Nicotiana attenuata*. Plant Cell *19*, 1096–1122.
57. Song, J., Bian, J., Xue, N., Xu, Y., and Wu, J. (2022). Inter-species mRNA transfer among green peach aphids, dodder parasites, and cucumber host plants. Plant Divers. *44*, 1–10.
58. Zhi, H., Chen, H., Yu, M., Wang, C., Cui, B., Zhao, X., Wang, Y., Cui, H., Zhang, B., and Zeng, Z. (2022). Layered double hydroxide nanosheets improve the adhesion of fungicides to leaves and the antifungal performance. ACS Appl. Nano Mater. *5*, 5316–5325.
59. O'Hara, R.B., and Kotze, D.J. (2010). Do not log-transform count data. Meth. Ecol. Evol. *1*, 118–122.

STAR★METHODS

KEY RESOURCES TABLE

REAGENT or RESOURCE	SOURCE	IDENTIFIER
Oligonucleotides		
Primers for PCR, quantitative real-time PCR and dsRNA synthesis see Table S1	This paper	N/A
Software		
SPSS (v. 16.0)	Kabak et al.[45]	https://www.ibm.com/de-de/spss
R (v. 4.0.2)	Alkarkhi et al.[46]	https://cran.r-project.org/
OriginPro (2023)	Munawar et al.[47]	https://www.originlab.com/
BioRender	Perkel[48]	https://www.biorender.com/
SigmaPlot (v. 14.5)	Bohoussou et al.[49]	https://systatsoftware.com/sigmaplot/
Inkscape (v. 0.48.2)	Minatani[50]	https://inkscape.org/
Chemicals		
Jarin-1 (JA-Inhibitor)	MedChemExpress	HY-115521; CAS: 1212704-51-2
SHAM (JA-Inhibitor)	Alfa chemicals	A736; CAS: 89-73-6
DIECA (JA-Inhibitor)	Alfa chemicals	711165; CAS: 148-18-5
AIP (SA-Inhibitor)	Alfa chemicals	A174; CAS: 141120-17-4
ABT (SA-Inhibitor)	Alfa chemicals	A126; CAS: 1614-12-6
Methyl jasmonate (MeJA)	Sigma-Aldrich	392707; CAS: 39924-52-2
Methyl salicylate (MeSA)	Damas-Beta	P1213257; CAS: 119-36-8
Salicylic acid (SA)	Sigma-Aldrich	SLBW0822; CAS: 69-72-7
Lanolin (Wool fat)	BBI chemicals	G518BA0024; CAS: 8006-54-0
Benzeneacetic acid	Cato chemicals	C3D-2629; CAS: 103-82-2
β-caryophyllene	Sigma-Aldrich	W225207; CAS: 87-44-5
Octanoic acid	Cato chemicals	CCFD200202; CAS: 124-07-2
Nonanoic acid	Cato chemicals	CCFD200192; CAS: 112-05-0
D-limonene	Sigma-Aldrich	BCBF5924V; CAS: 5989-27-5
ß-bisabolene	Cato Chemicals	CCPE901693; CAS: 495-61-4
Copaene	Sigma-Aldrich	HY-122485; CAS: 3856-25-5
Humulene	Sigma-Aldrich	PHL83351; CAS: 6753-98-6
Phenol	Sigma-Aldrich	P1037; CAS: 108-95-2
Nonanal	TCI chemicals	EXN8L-OF; CAS: 124-19-6
2-decen-1-ol	Sigma-Aldrich	669229; CAS: 4117-14-0
3-hexen-1-ol	Sigma-Aldrich	06104KD; CAS: 928-96-1
3-hexen-1-ol, acetate	TCI chemicals	BCCC1213; CAS: 3681-71-8
2-hexen-1-ol, acetate	Macklin chemicals	C10104671; 2497-18-9
ß-ocimene	Sigma-Aldrich	W353901; CAS: 13877-91-3
Germacrene D	Cato Chemicals	CCPE901491; CAS: 23986-74-5
2-hexen-1-ol, (E)	Macklin chemicals	C13585430; CAS: 928-95-0
(-)-ß-bourbonene	Sigma-Aldrich	CAS: 5208-59-3
(E)-α-bergamotene	Sigma-Aldrich	CAS: 18252-46-5
2-hexenal, (E)-	Macklin chemicals	1305L19; CAS: 6728-26-3

RESOURCE AVAILABILITY

Lead contact

Further information and requests for resources and reagents should be directed to and will be fulfilled by the lead contact, Wenwu Zhou (wenwuzhou@zju.edu.cn).

Materials availability

This study did not generate new unique reagents.

Data and code availability

All the data supporting the findings of this study are available within the paper and its supplemental information files.

EXPERIMENTAL MODEL AND SUBJECT DETAILS

Chemicals

Unless otherwise stated, all chemicals were purchased from Sigma-Aldrich, St. Louis, Mo.

Experimental plants and organisms

The potato plants used in this study were grown at Zhejiang University, Hangzhou, Zhejiang province of China. Plants were produced *in vitro* via tissue culture technique and grown at 20±1°C, 16 h light (100 μmol m^{-2} s^{-1}, LED T5 21W). Four–weeks after subculture, the plantlets were transferred to pots (diameter = 40 cm, volume = 1.5 L) filled with peat potting soil (Shenzhen Shenglvyuan Horticulture Co., Ltd, China). Plants were then grown in a glasshouse under 16h light (25±2°C) and 8h dark (20±2°C) with a light intensity of 600–800 μmol m^{-2} s^{-1} (600W, Lucagrow, Hungary) and were watered daily.[47]

Tetranychus urticae (TSM) adults were used as herbivores: the TSMs colony was established with ≥500 adults collected in a glasshouse at Zhejiang University, Hangzhou, China and maintained on potato plants in a climate chamber for more than four generations (25±2°C; 16 h:8 h L:D; 70% relative humidity). *Neoseiulus californicus* (PDMs) were used as predators of TSMs: PDMs were obtained commercially (Fuzhou Guan Nong Biological Science and Technology Co., Ltd. China) and a colony was maintained on TSMs hosts in a glass jar (1.5 L) in a climate chamber (25±2°C; 16 h:8 h L:D; 70% relative humidity). The opening of each jar was covered with mite-proof net to ensure proper ventilation and prevent mites from escaping.

METHOD DETAILS

PDMs preference and fitness tests

PDMs choice assays for flowers and TSMs

The plants with freshly opened flowers (~30 days after transplanting) were transferred into individual cages (45 × 65 × 75 cm). Plants were maintained with 5 flowers each; extra flowers and flower buds were removed before the experiment. Plant pots were covered with aluminum foil to minimize soil VOCs contaminating plant headspaces. About 30 PDMs adults collected in glass test-tubes (10 x 75 mm) were released at the stem base where they remained for 2 h (6 AM to 8 AM); stem bases were encircled with wet cotton to prevent mite escape, and the cotton was removed at 8 AM. Then PDMs numbers were immediately counted on leaves and flowers using a magnifying lens. Following treatments, another batch of plants (with PDMs pre-released for 2h) were infested with TSMs adults on leaves (100 adults per plant) for 2h (8 AM to 10 AM) and then the total number of PDMs on leaves and within flowers were counted. PDMs and TSMs were starved for 8h before experiments. To evaluate PDM floral preferences, 2 flowers harvested from insect-free plants and TSM-damaged plants were placed 7 cm apart in Petri dishes (15 x15 cm) into which 10 PDMs were released. PDMs recruited by flowers from TSM-induced or control plants were counted using a magnifying lens. To evaluate how long PDMs survive on potato plants lacking flowers and TSMs, 235 PDMs adults were released on each plant following the procedures described above. The number of PDMs remaining alive on each plant was counted using a magnifying lens at the designated intervals after release.

Anthers supplement and predation potential of PDMs

We determined the influence of anthers supplementation on PDMs prey consumption following the conditions previously described.[11] A small potato leaf disc (4 x 4 cm) was placed into a Petri dish (60 x 15 mm) surrounded with wet cotton to prevent mites from escaping. TSMs adults collected from the stock colony (25 adults/Petri dish) were placed on the leaf disc singly or in combination with anthers. Adult PDMs (10 adults/ Petri dish) were released into the Petri dish and allowed to feed for 24 h. The leaf discs were covered with a black plastic sheet to shelter the mites. TSMs consumed by PDMs within 24h was recorded. TSMs unable to move or missing body parts were considered predated.

Longevity and survival of PDMs with food substitution

The PDMs eggs collected from the stock colony under a microscope were transferred to a Petri dish (150 x 15 mm) for hatching (25±2°C; RH, 70%). Upon hatching, the newly emerged larvae (n = 20) were placed on a potato leaf disc (4 x 4 cm) and supplied with different foods. Experiments included four treatments: (**1**) -pollen -TSMs, (**2**) +pollen -TSMs, -pollen +TSMs, and (**4**) +pollen + TSMs. The total number of PDMs that survived were counted every two days and fresh diet was provided. TSMs adults were used as prey; 4 anthers harvested from freshly opened flowers provided the pollens.

Re–positioning of odors sources and PDMs movements tests

To evaluate if VOCs are involved in the distribution of PDMs among different plant organs, we manipulated the VOC bouquets of leaves or flowers using additional plants. Plants with uniform sizes and flower numbers were divided into two batches. With the first batch, plants were individually inoculated with 250 PDMs and left for 4h. With the second batch, plants were treated to manipulate

flower and leaves odors, elicited by TSMs, MeJA and MeSA treatments. To induce leaf VOCs, the individual compound leaves were elicited with TSMs infestations (n = 15 TSMs per leaflet), MeJA (7.5 uL/mL) and MeSA (7.5 uL/mL) treatments and immediately used in odor tests. The manipulated plants were introduced near the base of PDMs–infested plants (without touching) and PDMs distributions on leaves and flowers were counted after different time intervals. For TSMs odors, around 300 TSMs were transferred to sticky paper placed in a petri dish and introduced near the base of PDMs–infested plants using a stand. All odor–manipulated tests were repeated ten times.

PDMs olfactory tests

The choice responses of PDMs to flowers, intact leaves, or leaves induced with TSMs infestation were examined in a Y–tube olfactometer system (3.0 cm and 5.0 cm internal diameter at the entrance and two sidearms, respectively) comprising an entry arm (10 cm length) and two supporting arms (15 cm in length, 60° angle). The Y–tube was equipped with Y-shaped metal wire inside to facilitate the choice of PDMs, as previously explained,[51] following some modifications. The Y–tube was oriented horizontally and each of the choice arms were connected to a glass container (500 mL) containing odor sources via a Teflon tube. A small air pump (RESUN: 0.02MPa) was used to produce airflow through activated charcoal, distilled water and silica gel, while the air pressure was adjusted to 0.50 L min^{-1} calibrated by a flowmeter. The freshly-opened flowers and leaves were removed just before the test and maintained with moist cotton until use. Induced leaves were infested with TSMs (15 TSMs/leaflet) 2h before the tests. The starved PDMs adults were individually introduced at the entrance of the Y–tube and choices were recorded with mites crossed the score–line of the chosen arm. Every flower or leaf was used in ten releases and subsequently replaced with a fresh one; hence, 4–6 leaves or flowers were used per test.

In addition, we evaluated of the Y-tube olfactometer responses of PDMs to different synthetic plant VOCs. To assess responses, a filter paper (2 x 2 cm) containing diluted concentrations of selected VOCs was placed in a glass container (200 mL) connected to one of the choice arms, whereas a filter paper with solvent (n–hexane; ≥98.0%, Aladdin Industrial Corporation, China) was placed in another glass container, to serve as a control. The PDMs were introduced individually at the starting point of the arm and a choice was recorded when the mite crossed the score-line of the chosen arm. Each odor concentration was used to make ten releases. A standard curve was generated using a synthetic standard and plant–emitted β–caryophyllene levels to ensure that the applied concentrations were within realistic ranges[47] (Figure S2D). The relative peak area of β–caryophyllene in MS (mass chromatogram) was calibrated with serial dilutions (0.01 to 2 μL) of a β–caryophyllene standard and injected into a GC (gas chromatography) and extrapolating the sample concentrations from the standard curve. β–caryophyllene is a dominant volatile compound in leaves and flowers of *S. kurtzianum* and most potato cultivars (unpublished data). The connections of odor sources to the chosen arms were reversed after every 5–PDMs tested to avoid positional bias. After each test, the Y–tube and odor containers were washed (alcohol, 70%) and sterilized (120°C for 20 min). All the tests were performed in the dark.

Collection of plant VOCs

Trapping with Tenax–TA

The polyester cooking oven bags were used to cover a specific organ of a plant (flowers or leaves). The bags were equipped with two tubes in a row, a Teflon tube for air entrance and a Tenax–TA tube (SL–T002, Superlab) for air exit. A small air pump (0.02 MPa) was used to pump air through activated charcoal, distilled water, and silica gel to the polyester bag and then pumped into the Tenax–TA tube at 0.5 L/min. Several studies have recommended polyester bags as convenient enclosures of specific plant-parts during VOC collections.[52]

Sampling with PDMS tubes

The PDMS preparation and sampling of plant VOC from leaves and flowers were performed as previously described,[47,53] following slight modifications. In detail, for every biological replicate, one freshly opened flower was removed from the plant and incubated with PDMS tubes in sealed 22 mL glass vials (Agilent Technologies).[30] To determine the age effects on the intensity and quantity of floral VOCs released, flowers were removed from plants on different days after opening. To further characterize the VOCs emitted from different flower parts, a freshly opened flower was carefully dissected into sepals, petals, stigma and anthers with the help of forceps. Dissected parts were incubated with PDMS individually in 5 mL glass vials. To measure foliar VOCs releases, a compound leaf (3–4 leaflets) with PDMS was enclosed in a rectangular plastic box (10 x 10 x 3 mm). VOCs released from the stem and roots of the plants were captured by incubating the excised parts with PDMS in 22 mL and 500 mL glass vials, respectively. The detailed information on VOCs collection can be found in Figure S2. Exposed PDMS were returned to 1.5 mL sterile glass vials (Biosharp Life Sciences) using clean forceps and stored at –4°C until GC/MS analysis. Intact leaflets were used to collect constitutive VOCs releases. For induced VOC collection, the leaflets were infested with TSMs. Blank measurements with an empty plastic box or polyester bag were performed to identify VOCs derived from the sampling system.

VOCs analysis by TD-GC-MS

PDMS tubes were transferred into empty glass TD sampling tubes, which were conditioned prior in a thermal conditioner (SC-10, Superlab). The glass tubes or Tenax–TA tubes were placed individually in an autosampler with a thermal desorption unit (TD-100XR, Markes International), which was connected to a GC (Trace 1300, Thermo Scientific) and single quadrupole MS (ISQ 7000, Thermo Scientific) for analysis. The specifications for the column used, the desorption conditions and the spectra collections

and identification were as described previously.[53,54] Volatile peaks were identified and analyzed using authentic standards and the NIST v and rep libraries installed in the Chromeleon software v7.2.8 (Thermo Scientific, USA).

Legs' tips excised PDMs assays

The female adults of PDMs were placed individually on sticky paper and their abdomens were pressed to the sticky paper with a camel hairbrush. Sticky pieces were fixed on glass slides under a digital microscope camera (Nikon SMZ745T) coupled with a desktop. The terminal apotele segments of the first (I) or fourth legs (IV) were carefully removed using capillary glass tubes. The glass tubes were pre–heated to a reduced diameter (ID: 0.1–0.2, OD: 0.2–0.3). After the legs' tips were excised, the PDMs were carefully transferred to Petri dishes (15 x 30 mm) and fed TSMs. The PDMs that survived one day after legs-tips excision and moved freely, were chosen for the odor selection experiments.

Synthetic VOCs applications and PDMs behavior assays

To elucidate the roles of plant VOCs in PDMs movement, we applied synthetic VOCs to plant leaves and counted PDMs distributions on plant organs. Biologically-relevant concentrations (1.5 μL/mL) of selected VOC were dissolved in a liquified aliquot of lanolin (BBI Life Sciences). The lanolin aliquot was prepared as described previously.[55] Plants with freshly-opened flowers were transferred to individual cages (45 × 65 × 75 cm) and pots were covered with aluminum foil. Every plant was infested with 235 PDMs adults and left for 24h. The next day, the PDMs–infested plants were individually treated with lanolin + VOC paste on 2 fully-expanded mature leaflets with a spatula. The control plants were treated with pure lanolin. PDMs numbers were counted on the flowers and leaves using a magnifying lens.

Exogenous application of plant elicitors

To mimic plant–chemical defense responses, we applied methyl jasmonate (MeJA, 95%, Sigma), methyl salicylate (MeSA, 99%, Adamas) and Salicylic acid (SA, 95%, Sigma) to the plant leaves and flowers. Biologically relevant doses of MeJA, MeSA and SA diluted in liquified lanolin (BBI Life Sciences) were prepared the same day as their applications. The lanolin aliquot was prepared as described previously.[55] Glass scintillation vials (Agilent-Technologies) were filled with liquified lanolin (50°C water bath) and quantities of MeJA (7.5 μL/mL), MeSA (7.5 μL/mL) and SA (7.5 μL/mL) were added and mixed vigorously. We filled a plastic syringe (1 mL) with melted lanolin mixtures and aliquoted 0.02 mL droplets on wax paper or plastic sheets. The droplets were divided into half and each half was applied to a fully expanded leaf of plant or flower pedicels with a spatula or wooden sticks. Two leaflets per/compound leaf/plant were treated and smeared in the middle of the leaf (1 cm wide). Control plants were treated with pure lanolin.

Phytohormones extraction and quantification

The JA or SA contents were quantified from flowers and leaves of *S. kurtzianum* plants. Freshly-opened flowers were pooled from plants on different days of their openings. For each biological replicate, 3–4 complete flowers were used. For leaves, two fully–expanded compound leaves per plant were infested with TSMs (n = 15 TSMs per leaflet, 5–7 leaflets per compound leaf). After subsequent infestations, the TSMs were removed carefully with a camel-hair brush and two infested leaflets (one from each compound leaf) were harvested. The collected tissues of flowers and leaves were immediately flash–frozen in liquid nitrogen until analysis. Phytohormone extraction and quantification were performed on a UPLC-MS/MS system (LCMS-8040 system, Shimadzu) as previously described[56,57] without modifications.

Total RNA isolation and quantitative real-time PCR analysis

Plant RNA was isolated using Easy–Do Plant RNA Kit (TRIzol) following manufacturer instructions. The concentration and quality of RNA were determined using Thermo Fisher Scientific NanoDrop 2000. The Evo M–MLV RT Mix kit (Accurate Biotechnology Hunan Co., Ltd, China) was used to remove genomic DNA contamination from RNA and reverse transcribed to synthesize cDNA using T100™ Thermal Cycler (BIO-RAD, China) in a total volume of 20 μL. Quantitative real-time PCR analysis was performed on a Bio–Rad CFX96TM Real–Time PCR System (Bio-Rad Laboratories, CA) using SYBR Green Premix Pro Taq HS qPCR kits following manufacturer instructions. For each analysis, a four–point linear standard curve was constructed using a 1:10 dilution factor of a specific cDNA standard. The target gene transcript levels in all unknown samples were determined according to the standard curve. *Solanum kurtzianum eukaryotic translation initiation factor 3 subunit E* (*SkeIF3e*), a housekeeping gene, was used as an internal standard for normalizing cDNA concentration variations. For every treatment, 3–7 biological replicates were used. The forward and reverse primer sequences for SYBR Green–based quantitative real-time PCR are provided in Table S1.

Exogenous spray of chemicals

The leaves and flowers of *S. kurtzianum* plants were individually sprayed with SA and JA biosynthetic inhibitors. For detailed information about their chemical specifications, see key resources table. All five chemical solutions were diluted in distilled water containing 0.02% (vol/vol) Tween 20. The chemicals and the concentrations used are as follows: DIECA (100 μM), SHAM (200 μM), Jarin-1 (50 μM), AIP (50 μM) and ABT (100 μM). Distilled water containing 0.02% (vol/vol) Tween 20 and 0.01% ethanol was applied as a control treatment. The chemical treatments on leaves and flowers were performed on separate plants. The plants were sprayed for 24h following 6h intervals before the experiments. For flower treatments, immature flowers (flower buds) that would completely open after 24h were sprayed. For leaves, solutions were sprayed with a hand sprayer onto both surfaces of the leaves until run-off.

The plant's flowers or leaves were entirely covered with plastic sheets to avoid cross–contamination; these were removed immediately after spraying. As described earlier, sprayed plants were transferred into individual cages for VOCs collection, phytohormone analysis, and PDM behavioral tests.

Preparation and characterization of LDH nanosheets

MgAl–LDH nanosheets were prepared based on the co–precipitation methods as described[58] with slight modifications. Briefly, 0.1 M of magnesium nitrate hexahydrate ($Mg(NO_3)2 \cdot 6H_2O$) and 0.05 M of aluminum nitrate nonahydrate ($Al(NO_3)3 \cdot 9H_2O$) were dissolved in deionized water (200 mL) and stirred magnetically. Another aqueous solution (200 mL) containing sodium hydroxide (NaOH, 0.4 M) was poured slowly into the above solution and the reaction was vigorously stirred for 5 min. The resting precipitate was collected and washed repeatedly by re–dispersing in absolute ethanol and deionized water, followed by centrifugation. Finally, the product was carefully dried in a vacuum oven set to 65 °C for 12h, then ground into a fine powder and stored in a vial for further characterization.

The microscopic morphology, elemental distribution and crystal structure of the obtained sample were investigated by a scanning electron microscope (FE-SEM, ZEISS Gemini SEM300) coupled with an energy-dispersive X-ray spectrometer (EDS). Moreover, transmission electron microscope (TEM) images were recorded by an FEI Tecnai G2 F20 device. Powder X-ray diffraction patterns of the obtained nanosheet were examined with a Bruker D8 Advance diffractometer utilizing a Cu Kα radiation source ($\lambda = 0.154$ nm, $2\theta = 2^\circ$ to 80°) to study the sample's crystalline structures. The Fourier transform infrared spectroscopy (FT-IR) spectra were collected using a Thermo Fisher Nicolet Is50 spectrophotometer to analyze the functional groups on the sample's surface. Samples were placed in the sample compartment and scanned within wavenumbers ranging from 4000 to 400 cm^{-1} at a resolution of 4 cm^{-1}.

Designing and synthesis of dsRNA

The primers for dsGFP (double-stranded RNA targeting green fluorescent protein), dsAOC and dsEDS1 were designed based on the full–length open reading frame (ORF) sequence and used to synthesize dsRNA fragments. The interference fragments were not included in the quantitative real-time PCR to avoid their influence on transcription levels after RNAi. dsRNA was synthesized using the MEGAscript High Yield Transcription Kit (Invitrogen, China) according to the manufacturer's instructions. In detail, the DNA template for dsRNA synthesis was amplified with primers containing the T7 RNA polymerase promoter at both ends and the resulting purified DNA template was used to produce dsRNAs. The synthesized dsRNAs were purified through LiCl precipitation and re–suspended in nuclease–free water and the concentration of dsRNAs were measured with a NanoDrop 2000 (Thermo Fisher Scientific). Finally, the size and quality of the synthesized dsRNAs products were verified by 2% agarose gel electrophoresis.

dsRNA loading on LDH and spray applications

To define optimal and complete loading of respective dsRNAs into LDH nanosheets, the ratio of *in vitro* transcribed GFP–dsRNA (500 ng), AOC–dsRNA (500 ng) and EDS1–dsRNA (500 ng) were assayed at 1:1, 1:2, 1:3, 1:4, 1:5 and 1:10 (dsRNA–LDH (w/w)) multiple times. To load, dsRNA–LDH was incubated in a total volume of 20 μL at room temperature for 1 h with gentle orbital agitation (100 rpm). The complete loading of dsRNA was determined by the retention of dsRNA–LDH complexes in the well of a 2% agarose gel electrophoresis.[38] Appropriate loading ratios were unchanged, irrespective of the required scale–up volume. All treatment plants were grown in peat moss potting soil under glasshouse conditions (average temperature 25 °C) unless otherwise specified. The dsRNA-LDH treatments were conducted using a 1:6 dsRNA–LDH loading ratio. The controls used were water, LDH (0:6) and GFP–dsRNA (1:6). All plants (20 day old) were sprayed with an atomizer at approximately 100 μL per cm^2 of dsRNA-LDH on the leaf surface unless specified. The spray treatments were performed in the early morning before sunrise. Sprayed plants were analyzed for phytohormone levels, VOCs release, relative gene expression and PDMs behavioral assays tests, at day 10 post-dsRNA-LDH spray. The dsRNA-LDH-related experiments were repeated multiple times with similar results.

QUANTIFICATION AND STATISTICAL ANALYSIS

Statistical analysis of the data were performed using R (v.4.0.2),[46] SPSS 16.0 (SPSS Inc, New York, USA)[45] and Microsoft Excel. Graphs were prepared using MS Excel software (Office 365; Microsoft), R and Origin 8.5 (Origin Lab)[47] and SigmaPlot(14.5)[49] was used to generate the standard curve for BCP. Inkscape (v. 0.48.2) drawing tool was used to edit figures.[50] Descriptions of statistical analyses, sample numbers and biological replicates are provided in figure legends. The count data analyzed by GLM models were based on a Poisson distribution to account for the overdispersion of insects on plant organs, following the least square method (LSM) for pairwise comparisons.[59] Occasionally, the count data were displayed as percentage (%) in figures for better data visualization. The graphical illustrations were created with BioRender (https://biorender.com/).[48]